J. Mech. Phys. Solids 182 (2024) 105479

Contents lists available at ScienceDirect

Journal of the Mechanics and Physics of Solids

journal homepage: www.elsevier.com/locate/jmps

Asymptotically matched extrapolation of fishnet failure probability to continuum scale

Houlin Xu [a], Joshua Vievering [b], Hoang T. Nguyen [a,1], Yupeng Zhang [a], Jia-Liang Le [b], Zdeněk P. Bažant [c,*]

[a] Department of Civil and Environmental Engineering, Northwestern University, United States of America
[b] Department of Civil, Environmental, and Geo- Engineering, University of Minnesota, Minneapolis, United States of America
[c] Departments of Civil and Environmental Engineering, Mechanical Engineering, and Material Sciences, Northwestern University, 2145 Sheridan Road, CEE/A135, Evanston, IL 60208, United States of America

ARTICLE INFO

Keywords:
Failure probability
Probability distribution
Scaling
Size effect
Series and parallel connections
Extreme value probability
Continuum homogenization
Weibull distribution
Weakest-link model
Fiber-bundle model
Tail distribution
Monte Carlo simulations
Material architecture
Nacre
Octet spin-off

ABSTRACT

Motivated by the extraordinary strength of nacre, which exceeds the strength of its fragile constituents by an order of magnitude, the fishnet statistics became in 2017 the only analytically solvable probabilistic model of structural strength other than the weakest-link and fiber-bundle models. These two models lead, respectively, to the Weibull and Gaussian (or normal) distributions at the large-size limit, which are hardly distinguishable in the central range of failure probability. But they differ enormously at the failure probability level of 10^{-6}, considered as the maximum tolerable for engineering structures. Under the assumption that no more than three fishnet links fail prior to the peak load, the preceding studies led to exact solutions intermediate between Weibull and Gaussian distributions. Here massive Monte Carlo simulations are used to show that these exact solutions do not apply for fishnets with more than about 500 links.

The simulations show that, as the number of links becomes larger, the likelihood of having more than three failed links up to the peak load is no longer negligible and becomes large for fishnets with many thousands of links. A differential equation is derived for the probability distribution of not-too-large fishnets, characterized by the size effect, the mean and the coefficient of variation.

Although the large-size asymptotic distribution is beyond the reach of the Monte Carlo simulations, it can by illuminated by approximating the large-scale fishnet as a continuum with a crack or a circular hole. For the former, instability is proven via complex variables, and for the latter via a known elasticity solution for a hole in a continuum under antiplane shear. The fact that rows or enclaves of link failures acting as cracks or holes can form in the large-scale continuum at many random locations necessarily leads to the Weibull distribution of the large fishnet, given that these cracks or holes become unstable as soon they reach a certain critical size. The Weibull modulus of this continuum is estimated to be more than triple that of the central range of small fishnets. The new model is expected to allow spin-offs for printed materials with octet architecture maximizing the strength–weight ratio.

* Corresponding author.
E-mail address: z-bazant@northwestern.edu (Z.P. Bažant).
[1] Current affiliation: School of Engineering, Brown University, 184 Hope St, Providence, RI 02912, United States of America.

https://doi.org/10.1016/j.jmps.2023.105479
Received 30 August 2023; Received in revised form 16 October 2023; Accepted 28 October 2023
Available online 31 October 2023

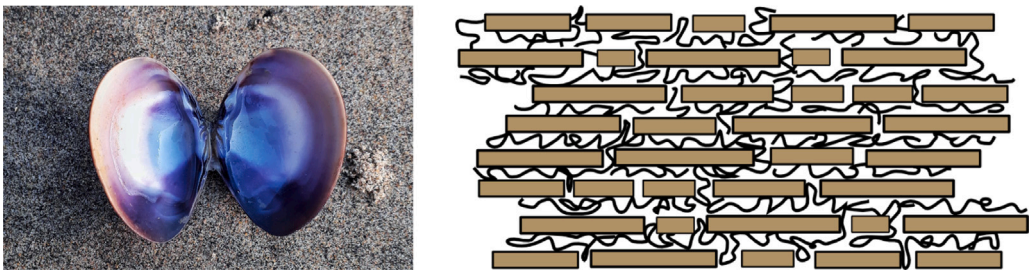

Fig. 1. (a) Internal image of a nacre shell whose micro-layered structure endows it with high strength. (From Unsplash: https://unsplash.com/s/photos/nacre); (b) Schematic illustration of the polymer linkage between structural layers of nacre (From Wikipedia: https://en.wikipedia.org/wiki/Nacre).

1. Introduction

Until 2017, there existed only two probabilistic models of structural strength:

(1) The series coupling model, a.k.a. the weakest-link model, which led in 1939 to the Weibull distribution at the large size limit (Weibull, 1939) (derived earlier by Fisher and Tippet in 1928 (Fisher and Tippett, 1928) without reference to material strength, as one of only three possible extreme value distributions; cf. Bažant and Le (2017) and Gumbel (1958)).

(2) The parallel coupling model, better known as the fiber bundle model, was shown in 1945 by Daniels (Daniels, 1945) to lead asymptotically to the Gaussian (or normal) distribution.

In 2017, it was found (Luo and Bažant, 2017a) that, with minor restrictions, an exact probability distribution can also be calculated for a system of regularly alternating series and parallel links, which is in nature exhibited, e.g., by nacre. Such a system resembles a diagonally pulled fishnet. It leads to what has been called *fishnet statistics*; see Luo and Bažant (2017a,b) where fishnets were analyzed for various sizes and various rectangular shapes (except very elongated and very wide ones). As it transpired, it suffices to consider that no more than 3 links fail up to the maximum load, P_{max}, which gives results very close to the structural failure probability for the case that any number of links can fail before P_{max}. This observation was confirmed by massive Monte Carlo simulations, consisting of one million runs for each fishnet geometry and each size. The results were ordered, inserted into boxes of equal intervals of the ordinate of the Weibull paper and averaged within each box. For small fishnets, each point represented on average about 10,000 Monte Carlo simulations (except for the tail points of distribution).

It has now been found, however, that the analytical results for the failure probability P_f of fishnets in which only 0, 1 or 2 links have failed up to reaching the P_{max} suffice to give good enough estimates of the actual P_f only when the number, N, of links does not exceed about 500 (one must exclude very elongated as well as very wide fishnets, which behave like a chain of links or like a fiber bundle). Beyond that, the analytical solution becomes too complicated and millions of Monte Carlo simulations for each case become unfeasible. Here we propose asymptotic matching to obtain an approximate, yet accurate, solution.

The effect of the size of geometrically scaled rectangular fishnets was previously decomposed into the effects of scaling up the width of the fishnet laterally, and of the length of the fishnet longitudinally (i.e., in the direction of loading). Both effects were then superposed to estimate the effect of the geometrically similar expansion of the fishnet (Luo and Bažant, 2020). This superposition, however, was an approximation. For the superposition to be exact, the lateral and longitudinal scalings would have to be statistically disjoint events, but this is not the case because parts of the laterally and longitudinally scaled rectangles overlap. The error of this simplification appeared to be significant.

Therefore, we take here a different approach and consider only geometrically scaled rectangular fishnets. We must also exempt from consideration fishnets of large width-to-length ratios which must approach the fiber-bundle model and must have a strength distribution that asymptotically converges to the Gaussian distribution.

2. Background of nacre strength prior to fishnet statistics

Over the past two decades, researchers have systematically studied the mechanics of nacre-like materials with 'brick-and-mortar' architecture in a deterministic framework (Fig. 1) (Wang et al., 2001; Gao et al., 2003; Barthelat, 2014; Yin et al., 2019; Barthelat et al., 2016; Bouville, 2020). The observed superior strength and fracture toughness of these materials can be attributed to the sliding behavior of the nano-asperities on the platelets (or lamellae) of hydrated nacre and the robust mechanical behavior on the macro-scale. It was shown that stress concentrations caused by intrinsic material flaws are inconsequential at the nano-scale (Gao et al., 2003). The staggered microstructure of nacre-like materials greatly enhances the fracture toughness of the material through the crack bridging mechanism.

By contrast, the statistical aspects of the failure of nacreous (or 'brick-and-mortar') structures have received much less attention, especially in regard to the tail behavior of the strength distribution. The failure statistics of quasibrittle structures under controlled loads is usually described by the weakest-link model, which features the damage localization mechanism. In the limiting case of an infinite number of links, the model leads to the Weibull distribution, which has commonly been assumed for strength distribution. However, the limitations of Weibull statistics for structural strength have long been realized.

The main issue is that, for many structures, the size of the material representative volume element (RVE) is not negligibly small as compared to the structure size, which invalidates the infinite weakest-link model. To address this issue, a finite weakest-link model was developed (Bažant and Pang, 2006, 2007; Bažant and Le, 2009; Le et al., 2009, 2011; Le and Bažant, 2011; Bažant and Le, 2017). The essence of the finite weakest-link model lies in the formulation of the strength distribution of the material RVE. The essential points are that: (1) the left distribution tail must be a power law of stress, which follows from Kramers' rule for the frequency of interatomic bond breaks, and (2) the failure of each RVE in progression from one scale to the next consists of both damage localization in the direction of tensile stress and load redistribution due to local parallel coupling in the transverse direction, which are features amenable to calculation of the cdf in transition from one scale to the next. Accordingly, the strength distribution of the macroscale RVE was statistically described by a hierarchical model of series and parallel couplings (Bažant and Pang, 2006, 2007; Le et al., 2011; Bažant, 2002; Le and Bažant, 2011).

The other statistical model that has been extensively studied is the parallel coupling model, aka fiber-bundle model. Unlike the weakest-link model, it takes into account the effect of stress redistribution. This model was first studied rigorously by Daniels (1945). He assumed equal load sharing among the elements or fibers acting in parallel and showed the distribution of the maximum load (or failure probability in the case of load control) to converge to the Gaussian distribution as the number of fibers tends to infinity (a proof for arbitrary postpeak softening of fibers is given in Bažant and Le (2017) below Eq. 5.5.3).

Later, a chain-of-bundles model was proposed by Harlow and Phoenix (1978a,b) for the failure probability distribution of fibrous composites under uniaxial tension. In that model, it was assumed that the specimen consists of a number of statistically independent cross sections, and each cross section was treated as a fiber-bundle for which a local load sharing rule was assumed. However, these assumptions were neither proposed nor justified from a mechanistic basis. Due to overwhelming obstacles for large-scale numerical simulations at that time, only bundles with less than 10 fibers were analyzed and no verification through Monte Carlo simulations could be given.

Recently, benefiting from the power of high-performance computing, one can simulate and analyze the interactions between individual components of large fishnets, taking into account factors such as material properties and applied forces. These simulations enable a deeper understanding of the structural integrity, load-bearing capacities, and potential failure modes of these fishnets, contributing to the design, optimization, and safety enhancement of large structures.

3. Decomposition of fishnet failure probability into a sum of disjoint events

It is convenient to express the strength distribution of the fishnet structure in the Weibull scale which is the scale in which the (two-parameter) Weibull distribution appears as a straight line, of slope equal to Weibull modulus, m. The coordinates of this scale are:

$$X = \ln \sigma_N, \qquad Y = \ln[-\ln(1 - P_f)] \tag{1}$$

where σ_N = nominal strength of structure = P_{max}/A, P_{max} = load capacity, A = cross-sectional area, measured homologously on geometrically similar structures, and P_f = cumulative distribution function of σ_N or equivalently the failure probability of the structure subjected to a nominal stress σ_N.

The failure probability P_1 of each link of the fishnet must be given as input. As explained in Luo and Bažant (2017b), it is taken in the form of a grafted Gauss–Weibull distribution. An exact analytical solution of a fishnet consisting of N links, each of which follows the Gauss–Weibull probability distribution, and whose failure occurs by a sudden stress drop, can be written as a sum of probabilities (Luo and Bažant, 2017b):

$$1 - P_f(\sigma) = P_{S_0}(\sigma) + P_{S_1}(\sigma) + P_{S_2}(\sigma) + \cdots \tag{2}$$

The terms of the sum represent the probabilities of the fishnet when 0, 1, 2, ... links fail before the maximum load, i.e., when the fishnet fails at the failure of one, two, three links, etc.; see Eqs. 1–3 and 13–16 in Luo and Bažant (2017a); see also (Luo and Bažant, 2017b, 2020). Obviously, these are disjoint events, which means that the individual failure probabilities must be summed, as in (2).

Evidently, the first term $P_{S_0}(\sigma)$ is exactly represented by the weakest-link model, i.e. $P_{S_0} = 1 - \left[1 - P_1(\sigma)\right]^N$. The second term P_{S_1} corresponds to the case where there is exactly one link failing at the peak load. The occurrence probability of this event (Luo and Bažant, 2017a,b) is given by

$$P_{S_1}(\sigma) = N P_1(\sigma) \left[1 - P_1(\eta_1 \sigma)\right]^{\nu_1} \left[1 - P_1(\sigma)\right]^{N-\nu_1-1} \tag{3}$$

where ν_1 = number of links that are close to the failed link and experience load redistribution with a factor of η_1.

For the third term, there are two failed links before the peak load. We may separate this case into two sub-cases: (1) the two failed links are adjacent to each other, and (2) the two failed links are far apart. The occurrence probability of the first sub-case, $P_{S_{21}}$, can be written as

$$\begin{aligned} P_{S_{21}} = N\nu_1 \int_0^\sigma \int_{x_1}^\sigma f(x_1) f(x_2) \mathrm{d}x_1 \mathrm{d}x_2 \left[1 - P_1(\sigma)\right]^{N-\nu_2-2} \left[1 - P_1(\eta_2 \sigma)\right]^{\nu_2} \\ + N\nu_1 \int_0^\sigma \int_\sigma^{\eta_1 \sigma} f(x_1) f(x_2) \mathrm{d}x_1 \mathrm{d}x_2 \left[1 - P_1(\eta_2 \sigma)\right]^{\nu_2} \end{aligned} \tag{4}$$

where ν_2 = number of the links that are close to the failed two links, η_2 = the load redistribution factor of these surviving links, and $f(x)$ = probability density function of the strength of the individual link. It is expected that $\eta_2 > \eta_1$.

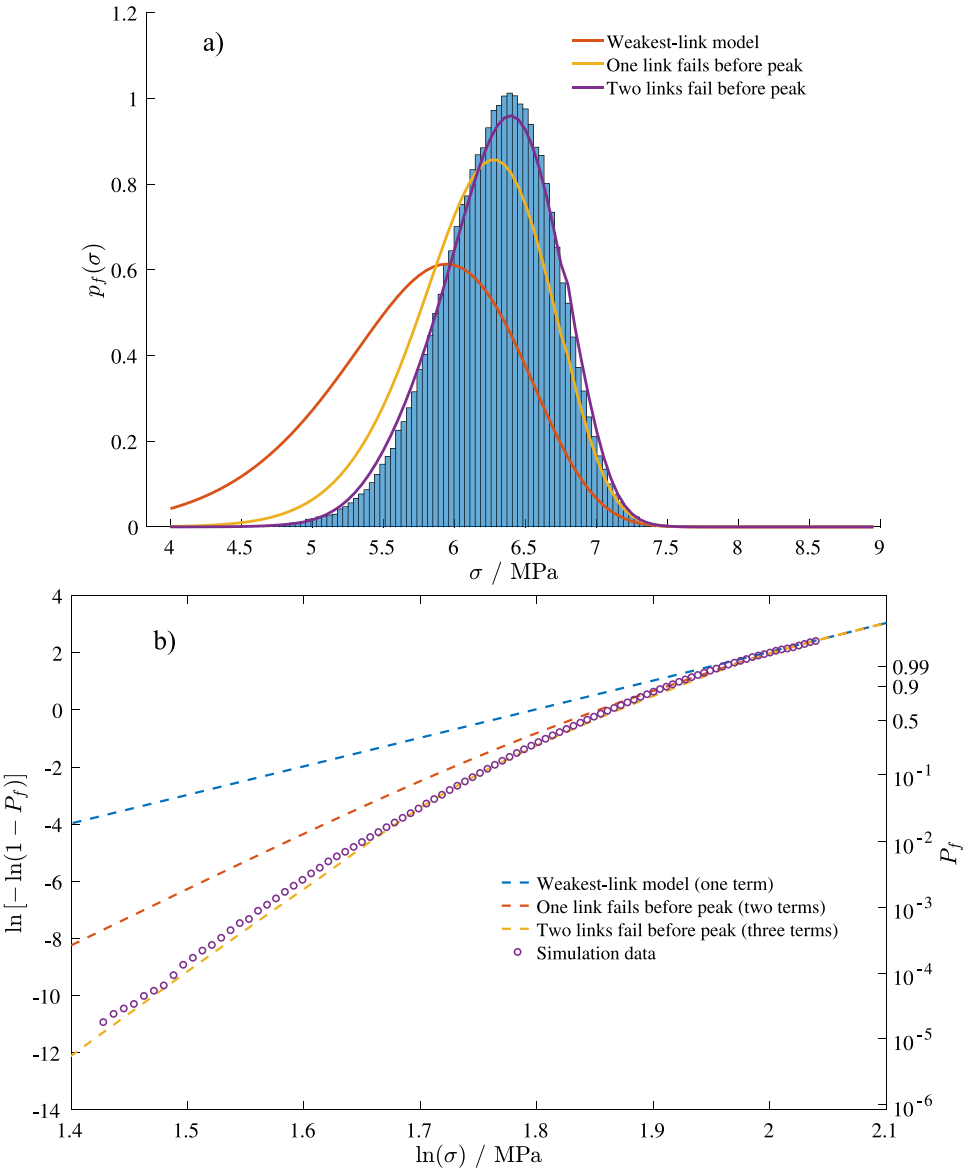

Fig. 2. Example of analytical solutions one term, two terms and three term failure probabilities compared with Monte Carlo simulations of a 10 × 38 fishnet.

Note that the first term of $P_{S_{21}}$ considers that the strengths of both failed links are smaller than σ, and so we need to consider the possibility that the strengths of the surviving links are smaller than σ. By contrast, the second term of $P_{S_{21}}$ considers that the strength of the first failed link is smaller than σ and the strength of the second one is between σ and $\eta_1\sigma$. It follows that the strength of the surviving links must be larger than σ. Therefore, in this case, we only need to calculate the survival probability of the links that are close to the two failed ones.

The occurrence probability of the second sub-case can be calculated as (Luo and Bažant, 2017a,b)

$$P_{S_{22}} = N(N-\nu_1-1)\int_0^\sigma \int_{x_1}^\sigma f(x_1)f(x_2)\mathrm{d}x_1\mathrm{d}x_2\left[1-P_1(\sigma)\right]^{N-2\nu_1-2}\left[1-P_1(\eta_1\sigma)\right]^{2\nu_1} \tag{5}$$

The first and second sub-cases are mutually independent, and so the probability P_{S_2} of having two failed links prior to the peak load can be expressed as a sum:

$$P_{S_2} = P_{S_{21}} + P_{S_{22}} \tag{6}$$

The analytical results for the first, second and third terms are shown in Fig. 2. As mentioned earlier, the term P_{S_0} is essentially the finite weakest-link model, which yields the Weibull distribution at the large-size limit. This distribution gives a straight line in

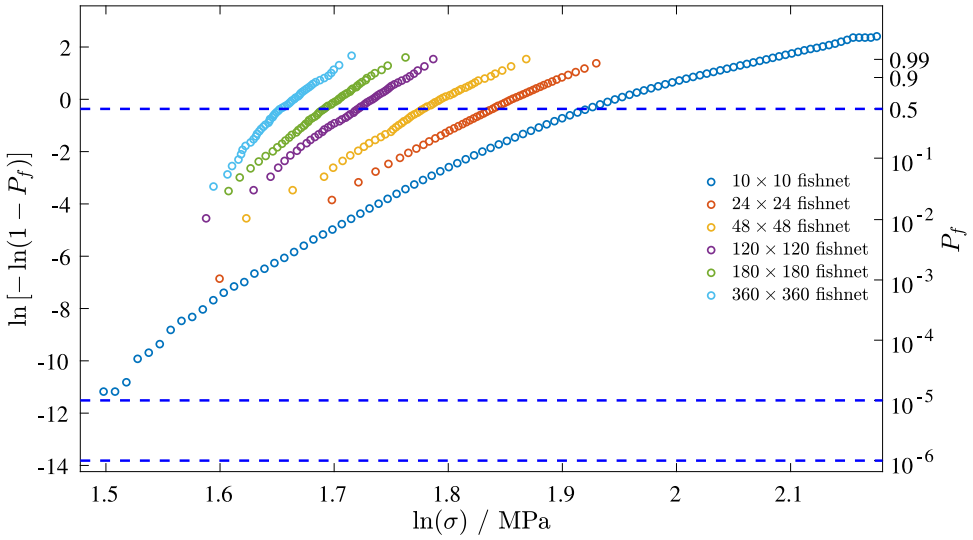

Fig. 3. Results of Monte Carlo simulations of fishnets of different sizes with (from right to left): $10\times10, 24\times24, 48\times48, 120\times120, 180\times180, 360\times360$ links.

Fig. 2. Its slope m equals the exponent of the power-law tail of the failure probability distribution of each link (the necessity of power law tail is a consequence of the Kramers' rule for interatomic bond breaks governed by activation energy (Bažant and Pang, 2006, 2007; Le et al., 2011; Xu and Le, 2018; Le and Xu, 2019)). The fact that on the far right the distribution must transit to Gaussian distribution curving to the right (as demonstrated in Bažant and Pang (2006, 2007) and Bažant and Le (2017)) is irrelevant for the present purpose and will be ignored here.

It may be noted that similar conclusions are obtained for fishnets whose links undergo gradual postpeak softening, which might be more realistic. In that case a different analytical approach is needed. The softening curve of each link is broken up into many subsequent softening jumps, which brings about one simplification and one complication. The simplification is that, if the softening jumps are small, no stress redistribution around the link with stress drop needs to be considered since the solution from the previous step suffices. The complication is that one must introduce order statistics, leading to geometric Poisson (Pólya–Aeppli) distribution of the number of clusters of damaged links (Luo and Bažant, 2018). Nevertheless, the overall behavior is similar as in the case of a sudden drop of stress in the links, and will not be here studied further.

Beyond the third term in Eq. (2), the analytical solution gets prohibitively complicated. Fortunately, though, the failure probability estimate up to the third term was, in the previous study, almost equal to the exact failure probability distribution, with any number of links failed before P_{max}, as shown by the last curve in Fig. 2. However, the present study revealed that this observation is true only for small rectangular fishnets with up to about 500 links, which merely suffice to characterize a representative piece of the real nacre shell. Excluded from the present analysis must be very wide but short fishnets which behave almost like the fiber bundle model and lead to a Gaussian distribution.

To extend the probability model to larger fishnets, we need an analytical description of the curves in Fig. 2, which we pursue next.

4. Approximate analytical model for P_f of fishnets extendable to large sizes

In this study, we investigate the strength distribution of large fishnets through Monte Carlo simulations of failure of square fishnets of different sizes ($10\times10, 24\times24, 48\times48, 120\times120, 180\times180, 360\times360$ links). Each link is considered to exhibit a perfectly brittle load–displacement response, i.e., the link loses its load carrying capacity immediately and completely once the peak load is attained. This is not the expected behavior of the linking polymer layer between the lamella of the nacre. Rather, a certain finite segment of this layer must get damaged before a crack within this layer runs through the whole length of the link layer. So, the failure of this connecting layer cannot be described by Weibull distribution since this distribution is valid only for an infinite weakest-link chain model (in practice a chain with more than about 10^5 links), for which the localized damage zone is negligibly small compared to the size of the link layer. The chain model is obviously finite, in which case the Weibull distribution transits for large stress to the Gaussian distribution (beginning with Weibull, such deviations from Weibull distribution have been mistakenly described by a three-parameter Weibull distribution with a finite threshold (whose error is evidenced by the size scaling properties)). So the failure of each interlaminar link must be described by the Gauss–Weibull distribution, developed and justified in Bažant and Pang (2006, 2007) and Bažant and Le (2017).

Note that the anisotropy of nacre does not invalidate the applicability of the present analysis to the loads in the plane (x, y) of nacre shell. But tension across that plane, normal to the lamellae of nacre, would not be describable by a fishnet. There may also be minor anisotropy between the x and y directions, but this is similar to the problem of biaxial tension.

The strength distribution of each link is described by the following grafted Gauss–Weibull cdf (Bažant and Pang, 2007; Bažant and Le, 2009; Le and Bažant, 2011):

$$P_1(\sigma) = \begin{cases} 1 - e^{-(\sigma/10.89)^{10}}, & \sigma \le 8.6\text{MPa} \\ 0.090 + \{0.436 - 0.474 \cdot \text{erf}[0.884(10 - x)]\}, & \sigma > 8.6\text{MPa} \end{cases} \tag{7}$$

where $P_g = 0.090$ is the grafting probability. Normally, for concrete, P_g is about 0.001; for nacre it was taken as 0.08. Here, the P_g must be higher because each link is not the RVE of the material but a structure itself. In nacre, the link represents the polymer layer which transmits shear and binds the adjacent stiff platelets. Thus the RVE of the link is much smaller than the length of the link (Bažant and Le, 2017, e.g.).

Following Luo and Bažant (2017b), for each realization we sample the random strength of each link independently of the Gauss–Weibull cdf, using the inverse-transform method. The specimen is loaded under uniaxial tension. During the loading process, an individual link is deleted from the specimen once its strength limit has been reached. The details of the element deletion procedure can be found in Luo and Bažant (2017b). A large number of realizations are performed to ensure that the simulated mean and standard deviation of the peak load capacity of the specimen converge within the relative tolerance of 1%.

The present Monte Carlo simulation considers the fishnet to be under uniaxial tension. How would failure probability change under biaxial tension? A major change is unlikely. What mainly matters is the topological connectivity of the links, i.e., the fact that the series and parallel links alternate. The links would no longer collapse into one line. The links would be inclined to the direction of both loadings, which would merely change the stress level. Uniform lateral tension would increase the stress level in all the links equally. All this would be equivalent to reducing the strength of the links, but would not change the distribution type. A more detailed demonstration may be of interest.

To formulate an approximate expression for P_f, we first analyze the asymptotic behavior of Eq. (2). Considering only the first term, we will get the Weibullian strength distribution if the specimen size is sufficiently large. In this study, since the power-law tail of the strength distribution of one link extends only to 10^{-2}, we expect to see the Weibull distribution for a fishnet consisting of more than 100 links. On the Weibull scale, this behavior is manifested by a straight line of slope m.

If we include the first two terms of Eq. (2) covering all the fishnet failures with no more than 2 links failed at P_{max}, we get the second curve from left in Fig. 2 which transits around the failure probability level of 10^{-3} to a straight line of slope $2m$. This asymptotic behavior can be shown mathematically by a binomial expansion of P_{S_0} and P_{S_1} and retaining all the terms up to the order $P_1^2(\sigma)$, i.e.

$$[1 - P_1(\sigma)]^N \approx 1 - NP_1(\sigma) + \frac{N(N-1)}{2}[P_1(\sigma)]^2 \tag{8}$$

$$\text{and} \quad P_{S_1} \approx NP_1(\sigma) - N(N - \nu_1 - 1)[P_1(\sigma)]^2 - N\nu_1 P_1(\sigma)P_1(\lambda_1\sigma) \tag{9}$$

By substituting these expansions into Eq. (2), we obtain

$$P_f = 1 - (P_{S_0} + P_{S_1}) \approx \left\{ N(N - \nu_1 - 1) - \frac{N(N-1)}{2} \right\} [P_1(\sigma)]^2 + N\nu_1 P_1(\sigma)P_1(\eta_1\sigma) \tag{10}$$

Since $P_1(\sigma) = (\sigma/s_0)^m$ for small σ, the two-term fishnet must have a power law tail with exponent $2m$. Combining the aforementioned behavior of the first term, we conclude that, on the Weibull scale, the two-term fishnet model will transit from a straight line of slope m to another straight line of slope $2m$ as the probability decreases. Physically it indicates that the probability of having two failed links at peak load is smaller than that of having one failed link.

We can extend this analysis to the three-term fishnet. In this case, we can perform binomial expansion of $P_{S_0}, P_{S_1}, P_{S_{21}}$ and $P_{S_{22}}$, and retain all the terms up to the order of $P_1^3(\sigma)$. This asymptotic analysis yields

$$\begin{aligned} P_f(\sigma) = \frac{N}{6}\left\{N^2 + 3\nu_1^2 - 3N - 3\nu_1 + 2\right\}[P_1(\sigma)]^3 - \frac{N\nu_1}{2}(\nu_1 - 1)P_1(\sigma)\left[P_1(\lambda_1\sigma)\right]^2 \\ - \frac{N\nu_1\nu_2}{2}P_1(\lambda_2\sigma)[P_1(\sigma)]^2 + N\nu_1\nu_2 P_1(\sigma)P_1(\lambda_1\sigma)P_1(\lambda_2\sigma) \end{aligned} \tag{11}$$

Evidently, the tail distribution of the three-term fishnet is a power law with an exponent of $3m$. It is now important to observe that, while proceeding in the Weibull scale downward (in the sense of decreasing probability), the three-term fishnet model produces a continuous transition through three straight-line asymptotes (or tangents) of slopes m, $2m$, $3m$) (intermediate in the sense of Barenblatt (1979)).

Fig. 3 presents the simulated strength distributions of square fishnets of different sizes. The results of the fishnet model as well as the Monte Carlo simulations indicate that, when we move down along axis Y in Fig. 3, the slope $\mathrm{d}Y/\mathrm{d}X$ for the smallest size fishnet is approximately incresed unformly for every certain orders of magnitude of P_f. Or, perhaps more accurately, for every decrease of $\Delta Y \approx -1$, the slope $\mathrm{d}Y/\mathrm{d}X$ is increased by 2.2. This conclusion remains applicable to other dimensions as well, although the precise numerical values may exhibit some variation. Based on the foregoing observations, we propose a linear increase of slope $\mathrm{d}Y/\mathrm{d}X$ in the negative Y direction and express it by the following differential equation:

$$\frac{\mathrm{d}Y}{\mathrm{d}X} = m'\left(1 - \frac{Y}{p}\right), \qquad X = \ln\sigma_N \tag{12}$$

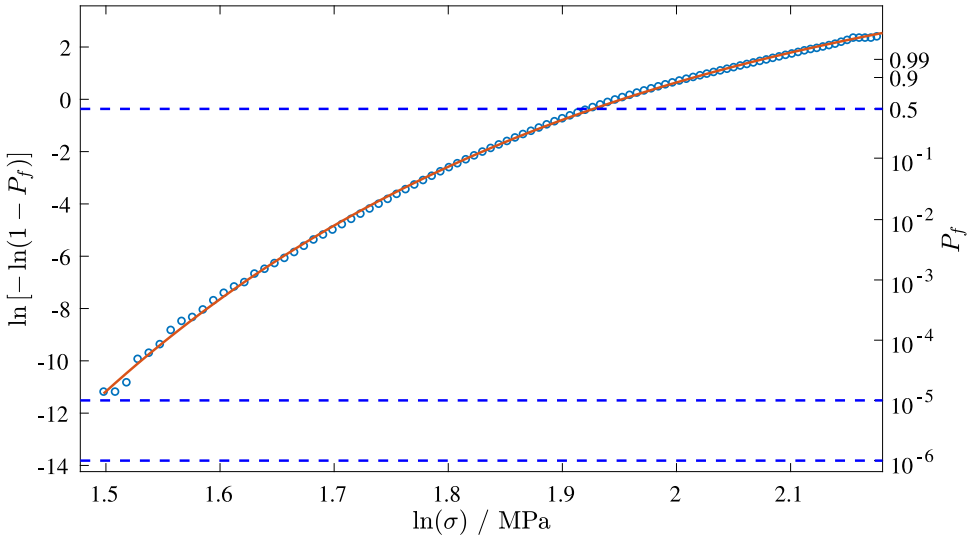

Fig. 4. Curve demonstrating close analytical fit (of Monte Carlo simulations of fishnets of size 10 × 10).

where p is a constant to be found. This equation can be easily integrated by parts: $Y = p - c_1 e^{-(m'X/p)}$ with c_1 as an integration constant to be found. The result is rearranged as

$$Y = p - \left(\frac{q}{\sigma_N}\right)^r, \quad r = \frac{m'}{p} \tag{13}$$

where $q = \ln c_1 / r$. Since the effective Weibull modulus, m', is not known *a priori*, we have three independent parameters, p, q and r (or m') to identify by data fitting.

To verify Eq. (13), we initially fit optimally the exact, analytically obtained, curves from Fig. 2, which themselves are in almost exact agreement with the massive Monte Carlo results. Here each point gives on the average about 10,000 to 20,000 data points in Weibull scale, albeit only few in the tails. The fit of the latter, shown by data points, is compared with the analytical optimum fit by Eq. (13), as shown in Fig. 4. We see that the optimum fit is very close. For one link we assume the exponent m of the power-law tail of strength distribution to be 10, and the parameters of the optimum fit then are:

$$p = 6.30, \quad q = 15.92, \quad r = 2.26 \qquad (m' = 14.24) \tag{14}$$

As will be seen, this equation matches the other cases of the present Monte Carlo simulations very closely. Hence, some underlying fundamental theoretical model ought to exist. But such a model is not yet clear. So we offer as least an explanation. Eq. (13) must be related to the decomposition into a sum of probabilities of disjoint events in Eq. (2). The slope increase with decreasing Y may be imagined as transitions from slope m' to $2m'$, from $2m'$ to $3m'$, etc. As already noticed in Luo and Bažant (2017b), the progressive slope increase corresponds to each additional term of the sum in Eq. (2) becoming significant, which in turn corresponds to the failures (or the P_{max}) occurring at the first, second, third, ... link broken. The failures at the first link break may be sufficiently characterized with 10^3 Monte Carlo simulations, which covers P_f up to 10^{-2}; the failures at the 2nd link break with up to 10^5 simulations, which covers P_f up to about 10^{-4}; the failures at the 3nd link break with up to 10^7 simulations, which covers P_f up to about 10^{-6}; etc. Obviously, addition of each next term in the sum, corresponding to each increment of the slope, results in a decrease of P_f by certain orders of magnitude. This decrease, as evident from the comparison of the vertical axes in Fig. 4, roughly corresponds to each increment of $\mathrm{d}Y/\mathrm{d}X$ due to negative ΔY in Weibull scale.

The decrease of the probability with adding more failed links can also be understood from the fiber-bundle model. The tail behaviors of the two-term and three-term fishnet models represent the failures of groups of two and three links, respectively. The formulation for calculating the failure probability of a group of two and three links is similar to the classical fiber-bundle model except that here we use different load sharing rules. Bažant and Pang (2007) studied the tail behavior of both brittle and plastic bundles, and showed that the probability at which the power-law tail terminates decreases approximately by two orders of magnitude when an additional fiber is added to the bundle. This is consistent with the aforementioned observation from the Monte Carlo simulations. This explanation, though, is not a rigorous proof.

5. Application to strength distribution of large fishnet

Two features change when we pass to fishnets containing much more than 500 links ($N \gg 500$): (1) Failures with more links broken before the maximum load become much more frequent and, in fact, dominate for very large N. (2) The number of Monte Carlo simulations must be reduced far below 10^6 because of computer time limitations. For fishnets consisting of about 10^5 links

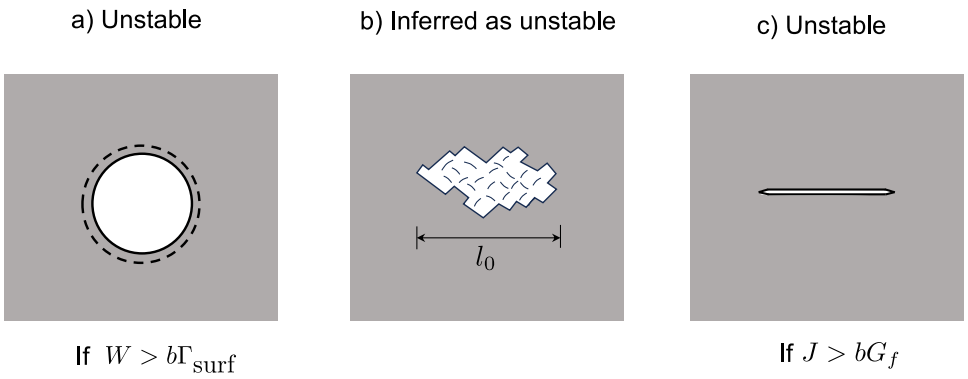

Fig. 5. (a), (c) Proven as unstable (i.e., failing) under controlled loads if the energy release rate, J, exceeds (a) the surface energy Γ_{surf} of the hole or (c) the fracture energy, G_f, of a crack (b = thickness in the transverse direction).

it was necessary to reduce the number of Monte Carlo simulations from 10^6 to 10^3. With this number of simulations one cannot ascertain failure probability $P_f < 0.01$.

Very large fishnets must approach a continuum. However, it is not a standard elastic continuum. Rather, as shown in Luo and Bažant (2017a), it is a continuum governed Laplace equation. Two limiting failure scenarios are identified:

1. An enclave of failed links forms and, under controlled loads, the structure becomes unstable when this enclave reaches a critical size, i.e. the applied load starts to decrease as the enclave grows further (Fig. 5a), see the Appendix.
2. The peak load is reached when a row of link fails, which resembles a single crack propagating in the fishnet. Depending on the fishnet boundary geometry (i.e., on whether the geometry is positive—see Appendix), the crack becomes unstable and runs dynamically as soon as it exceeds a certain critical length, just like in standard deterministic elastic continuum (Fig. 5c).

The actual failure behavior of the fishnet continuum should be in between them (e.g. Fig. 5b). In similarity to linear elastic fracture mechanics, we assume this to be approximately true also for the fishnet continuum. The reason is that the critical length of the initial crack, i.e., of the row of failed links, or the critical size of the enclave, is a material property, invariant with respect to the structure size. This implies that the number, k_1, of failed links within the critical crack length or within the enclave, representing the number of links that have failed up to the peak load, must be a constant.

It should be pointed out that, due to the randomness of strength of each link, there would be some failed links (let k_2 denote the number of these links) that are outside the main damage zone. The failure of these links must occur during the initial formation of the damage zone. This is because, as the damage zone grows, the stress concentration around the damage zone becomes significant, making it unlikely for further links far away from the damage zone to fail. It is thus reasonable to expect that, at the large size limit, k_2 becomes much smaller than k_1, allowing k_2 to be approximated by a constant.

In a macro-homogeneously stressed fishnet, such a damage row of failed links or an enclave of failed links leading to overall structural failure can occur at many possible locations. Any one of them can cause instability and dynamic failure of the whole fishnet. Such behavior is probabilistically equivalent to the weakest-link model, in which the failure of any link will cause overall failure. We note that the tail probability of the occurrence of the damage zone must follow a power law of link stress, with a constant exponent denoted as km, which equals to $k_1 + k_2$. In consequence, and also on the basis of the extreme value statistics (infinite weakest-link model), the failure probability distributions of a large fishnet (without a notch or preexisting crack) must be the Weibull distribution, which is a straight line in the (X, Y) plot.

The distinguishing characteristics of Weibull distribution implied by the infinite weakest link model are: (1) In 2D scaling, the mean strength of a two-dimensional (2D) specimen scales with the specimen size D by a power law of exponent $-2/km$, and (2) the coefficient of variation, C.o.V, of structure strength is a constant that is independent of the structure size and is determined solely by the Weibull modulus.

Fig. 6 shows the size effects on the mean and the C.o.V of the nominal structure strength. It is seen that both the mean and the C.o.V decrease with an increasing structure size. Though the size effect on the mean structure strength seemingly follows a power-law scaling for large fishnets, the C.o.V continuously decreases with the specimen size. This indicates that the strength cdf of the largest specimen considered in the simulation has not reached the Weibull distribution yet. In view of these considerations, we need to describe analytically the transition from small fishnets, $N < 500$, to very large fishnets, which obey the weakest-link model. This transition can be described with Eq. (12) by considering parameters m' and p to be size dependent. As $p \to \infty$, Eq. (12) predicts a constant slope, i.e., Weibull distribution of slope m'. Therefore, we expect that, as the specimen size increases, p would increase to a large value and m' would increase to km.

Fig. 7 shows that the Monte Carlo data can be fitted optimally by Eq. (12). This indicates the applicability of Eq. (12) for the large size range of the fishnet. Fig. 8 shows the dependence of parameters p and m' on the specimen size. Since the relationship is defined as $r = m'/p$, having knowledge of p, q, and r is adequate to establish the analytical solution. Notably, if we constrain p to adhere to the functional form $a \times e^{bx}$, a unique combination of p, q, and r emerges. The advantage here lies in the evident

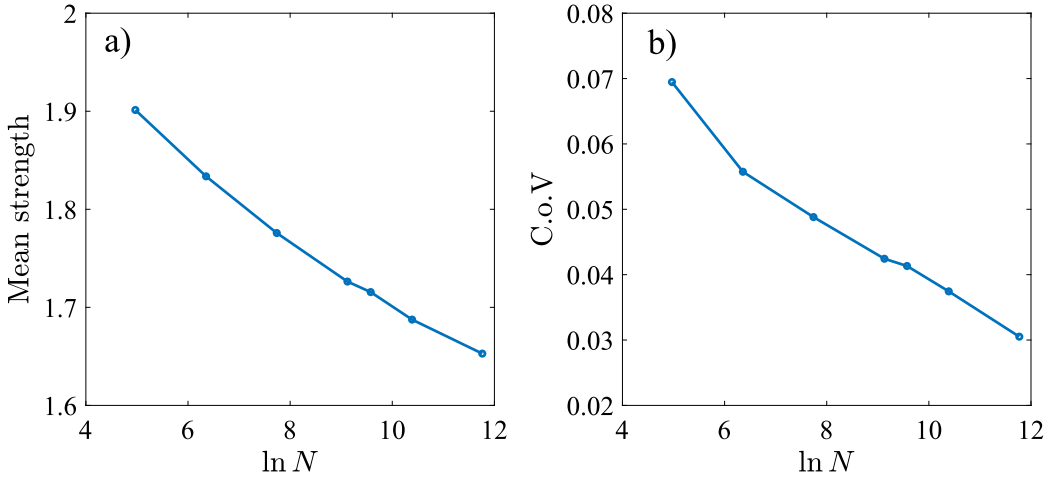

Fig. 6. Size effects on the mean and on the coefficient of variation (C.o.V.) of the nominal strength of structure.

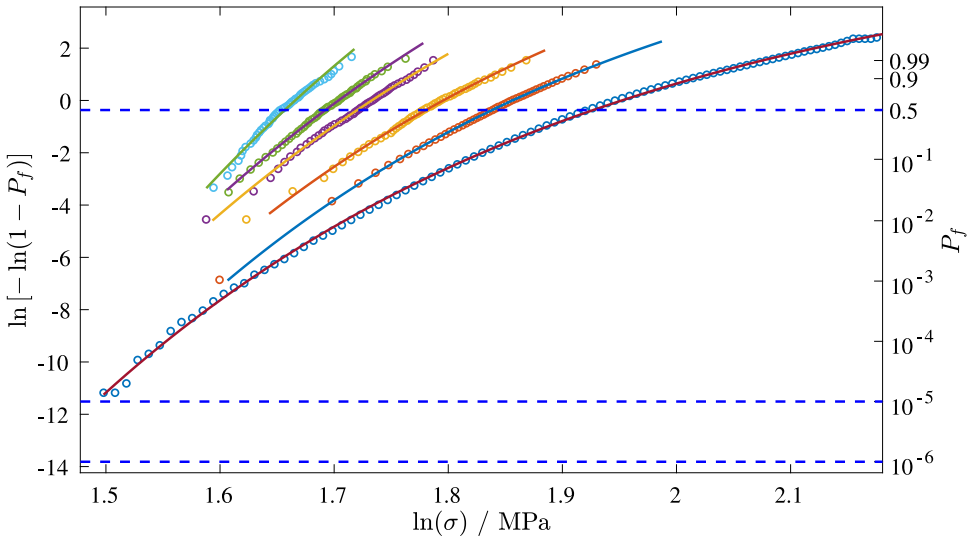

Fig. 7. Analytical fits of Monte Carlo simulations of failure probabilities of square fishnets of different sizes.

outcome that, as the scale increases ($\ln N \to \infty$), the right-hand side of Eq. (12) gradually stabilizes as a constant. Note that this size dependence would be different for different specimen geometries, i.e., the aspect ratios. The size dependence of m' is directly related to the damage pattern of the fishnet. Fig. 9 shows some simulated damage patterns of square fishnets of different sizes at the peak loads. These patterns are the typical results of Monte Carlo simulations. It is seen that, at peak load, a concentrated damage zone consisting of several links forms in the specimen. Meanwhile, there could also exist some isolated failed links in other parts of the specimen. As the loading proceeds, a row of links zips through from the damage zone. The key observation is that, for the range of the specimen sizes considered in the simulations, the number of failed links at the peak load increases with the specimen size. Therefore m' must increase with the specimen size.

In addition to the specimen size, the aspect ratio also influences the strength distribution. If the width-to-length ratio approaches infinity, the fishnet would behave as a fiber bundle. At the large-size limit, the strength distribution would then approach the Gaussian distribution. In the other extreme case, in which the width-to-length ratio approaches zero, the fishnet would behave as a chain leading to the Weibull distribution. The transition between these two limiting cases at varying aspect ratios is an intricate problem, which will require further investigation.

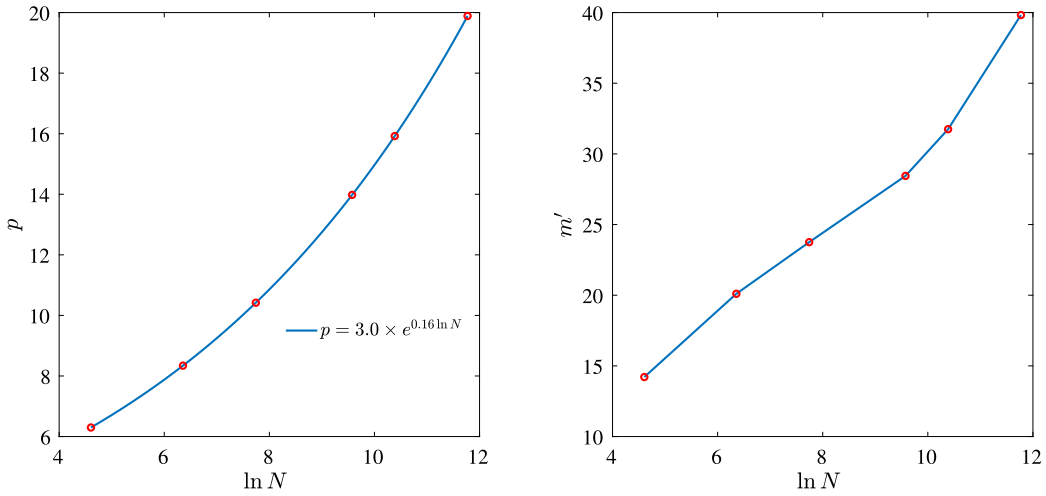

Fig. 8. Dependence of parameters p and m' on the specimen size.

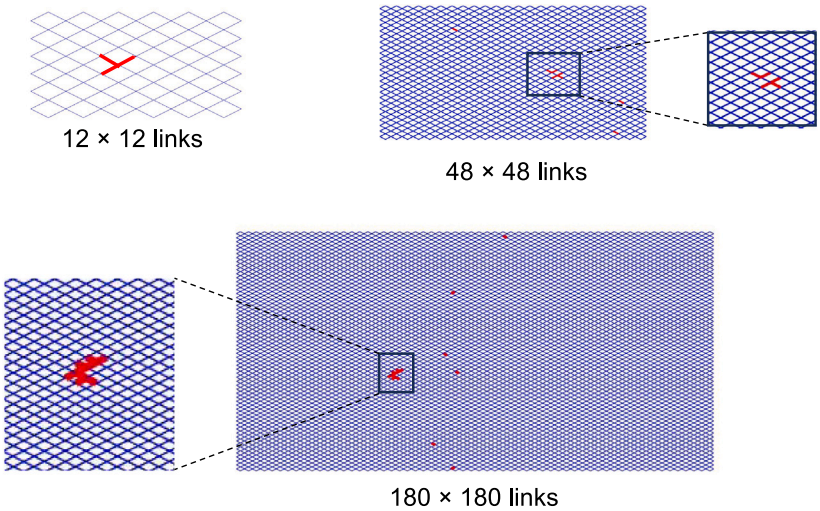

Fig. 9. Typical damage patterns of fishnets at the peak load.

6. The big picture

The original success of fishnet statistics (Luo and Bažant, 2017a,b, 2018) was to show that the microscopic brick-and-mortar architecture of nacre not only increases the strength and toughness in the mean, which was shown earlier (Gao et al., 2003; Tertuliano and Greer, 2016; Filleter et al., 2011), but also greatly increases the safety against overall failure in the sense of lowering the failure probability. The general wisdom of structural safety experts is that engineering structures such as bridges, aircraft or computer chips are "safe" if their failure probability is less than 10^{-6} (which is roughly the probability of being killed by a falling tree, lightning or wild animal).

The fishnet architecture of alternating series and parallel connections causes the nominal stress σ_N with failure probability 10^{-6} to be about 50% farther from the mean than it is for the Gaussian (or normal) distribution (the Gaussian is exact only for the fiber bundle model, i.e., for a parallel coupling architecture). So, taking advantage of the 50% enhancement leads to safer structural design.

It should be highlighted that, beyond its widely recognized exceptional average strength, the nacreous architecture offers a significant additional benefit in the extremely low probability range. In contrast to the linear Weibull distribution with slope m in the (X, Y) plot, which is observed in materials such as fine-grained ceramics and is often indiscriminately used for all brittle fracture, there is a notable disparity between the points where the horizontal line of Y corresponding to $P_f = 10^{-6}$ intersects the Weibull straight line and the computed curve for the fishnet. This disparity demonstrates that at $P_f = 10^{-6}$, the strength in the tail

is augmented by 72% compared to the Weibull distribution. This is a remarkable enhancement of safety, gained by the nacreous architecture.

A similar analysis has been carried out in Luo and Bažant (2020) for the octet material architecture. The octet is attractive as a printed material of a very high strength–weight ratio. As it transpired, it essentially represents a generalization of two-dimensional fishnet to three dimensions (in fact, the octet can be decomposed into three planar fishnets of different orientations (Luo and Bažant, 2020)). The Monte Carlo simulations in Luo and Bažant (2020) showed that the aforementioned distance of the octet probability distributions from the mean is even higher than it is for the fishnet. In other words, the octet is even safer than the fishnet.

Fishnet statistics cannot be applied to particulate quasibrittle materials such as concrete. But the pure Weibull statistics does not seem to apply perfectly. Statistical data showing whether the C.o.V of strength may be constant for a broad range of sizes are unavailable. Nevertheless, recent computer simulations of force chains in concrete under uniaxial tension show (Tejchman et al., 2013) that adjacent longitudinal tensile force lines cross, which means that lateral force transmissions between adjacent parallel tensile force chains exist. This suggests that only a certain percentage, say 90%, of the links simulating the failure statistics of concrete act as series couplings while the remaining 10% might act as parallel couplings. This suggests a deviation in the upper tail from the Weibull distribution toward the Gaussian distribution. How to treat it probabilistically is a challenge.

The probability of material strength, or non-failure, is, or course, only one of two aspects of structural safety, which underlies the capacity reduction factors, popularly called the 'understrength' factors. The other aspect is the probability of loads, which underlies the load factors used in design. The understrength factors have so far been mostly empirical and represent the weaker part of the joint probability of failure which has so far received far less attention. It should be realized that the failure probability of 10^{-6} cannot be assessed empirically.

The failure probability of structures is an integral of the joint probability of (i) the loads of various types and (2) the structure strength. The probability of the former has been studied far more than of the latter, and is now much better understood. The latter has so far been handled in practice by empirical 'understrength' factors. But their dependence on the material architecture, microstructure and constituents is generally a woefully underexplored subject. This study aims to make a step toward remedy.

7. Conclusions

1. The recently developed fishnet statistics is limited to systems with less than about 500 links.
2. The approximation of exact failure probability distribution for small fishnets with up to three failed links in a row at maximum load, confirmed by massive Monte Carlos simulations with about a million runs per case, is sufficient to establish in a simple way the failure probability down to about 10^{-5}.
3. A differential equation is derived for the evolution of probability distribution of fishnets of various sizes.
4. The likelihood to have more links failing at the peak load increases with the size of the fishnet specimens. At the large size limit, the total number of failed links at the peak load appears to approach a constant. This implies that the strength cdf of the fishnet should asymptotically converge to the Weibull distribution.
5. Solving the Laplace equation for a continuum fishnet with a crack (Fig. 5c) by means of complex variables shows that a fully formed crack of sufficient size at any interior location makes a large rectangular fishnet unstable. A known elasticity solution for a continuum proves the same for a circular hole (Fig. 5a) at any location. We assume this to be also true for an irregular enclave of failed links (Fig. 5b), which is an intermediate case between a crack and a hole.
6. Like the size of a crack or hole, the size of the enclave of failed links sufficient to cause failure is considered to be a material property of the fishnet, invariant with respect to the structure size. This further implies that the number, k_1, of failed links within the enclave must be a constant (Fig. 5b).
7. Asymptotic matching of the failure distribution of small and large fishnets yields a general formula for estimating the fishnet failure probabilities up to 10^{-6}. But fishnets very wide laterally must be excepted.

CRediT authorship contribution statement

Houlin Xu: Mathematical formulation, Computer simulation, Data analysis, Help in writing, Checking the text. **Joshua Vievering:** Computer simulations, Statistical parameters, Checking the text. **Hoang T. Nguyen:** Checking early computations, Checking the text. **Yupeng Zhang:** Helping computer simulations, Checking the text. **Jia-Liang Le:** Conceived mathematical formulation, Updated paper text, Checking the text. **Zdeněk P. Bažant:** Original concept of mathematical formulation, Original paper text, Checking the text.

Declaration of competing interest

The authors declare that they have no known competing financial interests or personal relationships that could have appeared to influence the work reported in this paper.

Data availability

Data will be made available on request.

Acknowledgments

Z. P. Bažant acknowledges partial financial support under ARO, United States of America grant W911NF-19-1-003 to Northwestern University, and J.-L. Le acknowledges partial financial support under the National Science Foundation , United States of America grant CMMI 2151209 to the University of Minnesota. Thanks for the valuable discussions that are due to Dr. Wen Luo, a postdoctoral associate at Caltech, formerly a doctoral student at Northwestern, and currently an Assistant Professor of Aerospace Engineering at Auburn University.

Appendix. Stability of a crack or hole in rectangular fishnet continuum

Near-tip field of a crack in fishnet continuum

We have tacitly assumed that a crack consisting of a row of sufficiently many broken links in a fishnet continuum becomes unstable as soon as fully formed. If there is a large zone under macro-uniform stress, the failure can initiate at many places and the material strength is random, such behavior inevitably leads to the Weibull distribution and Weibull size effect as the structure size is scaled up, which is what we considered. But this behavior should be mathematically proven, which we do next.

The equilibrium condition of node (i,j) of a fishnet collapsed into a line in the x direction is

$$F_{i,j+\frac{1}{2}} - F_{i,j-\frac{1}{2}} + F_{i+\frac{1}{2},j} - F_{i-\frac{1}{2},j} = 0 \tag{15}$$

where $F_{i,j+\frac{1}{2}} = (EA/l)[u_{i,j+1} - u_{i,j}]/l$, etc.; E, A = Young's modulus and cross section areas of the links and l = their lengths; $u_{i,j}$ are the nodal displacements; i = 1,2,3, ...= node numbers in the link direction ξ of fishnet before collapse into a line and j = 1,2,3, ...= node numbers in the link direction η. Eq. (15) represents a difference equation whose continuum approximation is $\partial^2 u/\partial\xi^2 + \partial^2 u/\partial\eta^2 = 0$ or

$$\nabla^2 u = 0 \tag{16}$$

which is the Laplace equation, as shown in Luo and Bažant (2017a). Since the Laplacian is invariant at coordinate rotations, this equation also applies in coordinates x, y, i.e., $\nabla^2 u = \partial^2 u/\partial x^2 + \partial^2 u/\partial y^2 = 0$ (note that these x, y directions have nothing to do with the link directions $\pm 45°$ before the fishnet was allowed to collapse into one line under tension). In the collapsed state, the coordinates of subsequent nodes $m = 2, 4, 6, \ldots$ along one link line are $y_{2m} = 2m\nu h$ where $\nu = 1/\sqrt{2}$. In the transverse direction, coordinate y measures the transverse distance before fishnet collapse into one line. After fishnet collapse, we have $x_{2n} = 2n\nu h$ for the subsequent lines. Thus the meaning of coordinate x is to serve as a counter of the link lines collapsed into one line, and so n = integer part of $(x/2h\nu)$.

The continuum approximations of axial forces and stresses in the links whose initial directions were x and y are

$$F_x = A\sigma_x, \quad F_y = A\sigma_y \tag{17}$$

$$\sigma_x = Eu_{,x}, \quad \sigma_y = Eu_{,y} \tag{18}$$

where subscripts preceded by a comma denote partial derivatives. Note that the stresses and strains in a fishnet continuum are vectors, not tensors. The strain energy density $\bar{U} = AU$ where U = strain energy density per unit area A and is expressed as $U = \frac{1}{2}E(u_{,x}^2 + u_{,y}^2) = \frac{1}{2}E\,u_{,i}u_{,i}$ where $i = 1, 2, j = 1, 2$ now represent the numerical subscripts referring to coordinates x, y before fishnet collapse, and the summation convention applies for the indices. The forces in the links are $F_x = A\sigma_x, F_y = A\sigma_y$, and the stresses in the links may now be expressed as

$$\sigma_x = \frac{\partial U}{\partial u_{,x}}, \quad \sigma_y = \frac{\partial U}{\partial u_{,y}} \qquad \text{or} \qquad \sigma_i = \frac{\partial U}{\partial u_{,i}} \quad (i = 1, 2) \tag{19}$$

To deal with the singularity near the tip of a sharp crack in direction x, we introduce polar coordinates (r, θ), in which

$$\nabla^2 u = u_{,rr} + r^{-1}u_{,r} + r^{-2}u_{,\theta\theta} \tag{20}$$

It can be shown (similar to Bažant et al. (2021)) that the asymptotic stress field near the crack tip must have the separated form

$$u = r^\lambda f(\theta) \tag{21}$$

Substitution into Eq. (20) yields the differential equation for function $f(\theta)$:

$$f'' + \lambda^2 f = 0 \tag{22}$$

where $f'' = \mathrm{d}^2 f/\mathrm{d}\theta^2$. The general solution is $f(\theta) = B\sin\lambda\theta + C\cos\lambda\theta$, with arbitrary constants B, C. The solution must obviously be symmetric in y with respect to the crack extension line $y = 0$, i.e., $f(\theta) = f(-\theta)$, and so $C = 0$. To determine B, we use the boundary condition of vanishing stress at crack surface, $[\sigma_y]_{y=0} \propto [u_{,\theta}]_{\theta=\pi} \propto f'(\pi) = 0$, which gives the condition $B\lambda\cos\lambda\pi = 0$. Since vanishing B and λ are physically unacceptable, the smallest possible solution is $\lambda\pi = \pi/2$, i.e.,

$$\lambda = \frac{1}{2}, \qquad f(\theta) = B\sin\frac{\theta}{2} \tag{23}$$

Therefore the stresses have the usual $-1/2$ singularity,

$$\sigma_r = \frac{K}{\sqrt{r}} \sin\frac{\theta}{2}, \quad \sigma_\theta = \frac{K}{2\sqrt{r}} \cos\frac{\theta}{2} \tag{24}$$

where K is a constant of metric dimension $\mathrm{N/m^{-3/2}}$, which needs to be determined from the boundary conditions. It will be called the fishnet stress intensity factor, like in linear elastic fracture mechanics (LEFM)

Note that the result $\lambda = 1/2$ also confirms the physical requirement that the work W of stress σ_x on the crack opening displacement Δu must be finite. Indeed, $W \propto \sigma_x \Delta u \propto r^{\lambda-1} r^{\lambda}$, and so W is nonsingular if $r^{2\lambda-1}$ or $2\lambda - 1 = 0$, or $\lambda = 1/2$. This is an alternative, energetic, derivation of the λ value.

We will consider rectangular fishnets with fixed boundary conditions, $u = 0$. At the free boundary parallel to axis y (i.e., x = constant), we have, before the fishnet collapses into a line, $(EA/h)[(u_{i+1,j} - u_{i,j}) + (u_{i,j-1} - u_{i,j} - u_{i,j-1})] = F$ where $F = A\sigma$ is the force applied at boundary node (i, j). The continuum approximation is $\partial u/\partial\xi - \partial u/\partial\eta = 0$. Transformation to coordinates $x = (\xi + \eta)/h$, $y = (\eta - \xi)/h$ yields the boundary condition:

$$u_{,x} = \sigma/E \qquad \text{(B.C. along } x = \text{const.)} \tag{25}$$

At the load-free boundary, one similarly obtains:

$$u_{,y} = 0 \qquad \text{(B.C. along } y = \text{const.)} \tag{26}$$

Crack in infinite fishnet continuum solved by complex variables

Here we consider the failure of fishnet to be caused by the formation of a single crack, as one possible limiting failure scenario. The problem of a crack in Laplace equation is analogous to an antiplane (Mode III) shear crack in elastic continuum, which itself is analogous to incompressible laminar flow past a sharp edge, and has been solved long ago (Eqs. 3.9.1–3.9.5 in Knott (1973); Eq. 4.3.36 in Bažant and Planas (1998); also (Barenblatt and Cherepanov, 1961)). The crack, of length $2a$, is normal to the load direction, now labeled as y, and is parallel to the transverse axis x. Complex variables offer an effective approach since the real (as well as imaginary) part of every analytic function $f(z)$ of complex variable z is a harmonic function, i.e., satisfies the Laplace equation. Thus the opening profile of the crack is expected to be a quadratic function—an ellipse: $u = (\sigma/E)\sqrt{a^2 - x^2}$ if $|x| \le a$. Accordingly, we assume the complex displacement to have the form

$$u = (\sigma/E)\sqrt{a^2 - z^2}, \qquad z = x + iy \tag{27}$$

where $i^2 = -1$. Calculation of the complex displacement gradients then yields $u_{,x} = \frac{1}{2}(\sigma/E)(a^2 - z_2)^{-1/2}(-2z)$, $u_{,y} = \frac{1}{2}(\sigma/E)(a^2 - z^2)^{-1/2}(-2z)i$. Hence,

$$\sigma_x = Eu_{,x} = -\frac{\sigma z}{\sqrt{a^2 - z^2}}, \quad \sigma_y = Eu_{,y} = \frac{\sigma z}{\sqrt{z^2 - a^2}} \tag{28}$$

Note that, in the fishnet continuum, the stresses are vectors.

The boundary conditions at infinity are satisfied because, according to Eq. (27),

$$\mathrm{Re} \lim_{|z|\to\infty} Eu_{,x} = \mathrm{Re}(i\sigma) = 0, \quad \mathrm{Re} \lim_{|z|\to\infty} Eu_{,y} = \sigma \tag{29}$$

where σ is the stress applied at infinity. The displacement boundary condition on the crack line, $y = 0$, outside the crack, is $\mathrm{Re}\, u = 0$. Indeed, from Eq. (27),

$$\mathrm{Re}\, u = \mathrm{Re}\, \frac{i\sigma}{E}\sqrt{x^2 - a^2} = 0 \quad \text{for} \quad |x| \ge a \tag{30}$$

The boundary condition of zero stress on the crack surface is also satisfied;

$$\sigma_y = -\mathrm{Re}\, Eu_{,y} = \mathrm{Re}\, \frac{\sigma x}{i\sqrt{a^2 - x^2}} = 0 \quad \text{for} \quad |x| < a \tag{31}$$

Further note that

$$\mathrm{Re}\,|u|_{y\to\infty} \;\to\; \frac{\sigma}{E} y, \quad \mathrm{Re}\,|u|_{x\to\infty} \;\to\; \mathrm{Re}\, \frac{\sigma}{E} ix = 0 \tag{32}$$

which means that the boundary condition at $y \to \infty$ is also compatible with a rigid boundary plate sliding in x direction and displaced in y direction.

To check the singular field near the crack tip, we may introduce the coordinate $r = x - a$ measured from the crack tip. From Eq. (28), for $x \ge a$ or $r \ge 0$, with r measured along the crack line,

$$Eu_{,x} = \frac{-\sigma(r + a)}{\sqrt{(r + 2a)r}}, \quad Eu_{,y} = \frac{-\sigma(r + a)}{\sqrt{r(2a - r)}} \tag{33}$$

$$\text{for } r \ll a: \quad Eu_{,x} = -\sigma\sqrt{\frac{a}{2r}}, \qquad Eu_{,y} = \sigma\sqrt{\frac{a}{2r}} \tag{34}$$

These equations agree with Eq. (24) and provide the stress intensity factor definition:

$$K = \sigma\sqrt{2a} \tag{35}$$

Crack instability in fishnet of positive geometry

Similar to LEFM, the critical value $K = K_c$ at which the crack can propagate through the fishnet continuum must be regarded as a material property (probably restricted to negligible crack-parallel stress (Bažant et al., 2021; Nguyen et al., 2020b,a)). For $K < K_c$, the crack cannot propagate. The case $K > K_c$ is unstable and leads to dynamic propagation. Similar again to LEFM, the structural geometry for which

$$\left[\mathrm{d}K/\mathrm{d}a\right]_\sigma > 0 \tag{36}$$

is called the case of positive geometry of the structure. In deterministic analysis, a spontaneous increment δa will increase K above the critical value K_c, which inevitably causes dynamic crack growth and failure. In stochastic analysis, one may consider K_c to exhibit spatial randomness described by a random field $K_c(x)$. The instability condition can then be expressed by

$$K = K_c \quad \text{and} \quad \left[\mathrm{d}K/\mathrm{d}a\right] > \left[\mathrm{d}K_c(x)/\mathrm{d}x\right] \tag{37}$$

Therefore, depending on the spatial variation of random fracture toughness, instability could occur at a finite crack growth. If the random field $K_c(x)$ has a sufficiently long autocorrelation length, one would expect the local spatial variation of $K_c(x)$ would be minimum (i.e. $\mathrm{d}K_c/\mathrm{d}x \approx 0$), and therefore Eq. (37) would essentially be the same as Eq. (36).

According to Eq. (35), the positive geometry condition is obviously satisfied for an infinite fishnet, and because continuity is expected, it must also be satisfied for sufficiently large fishnets. That it is satisfied for finite rectangular continuous fishnets is likely but, of course, not proven. An analytical proof may be tedious and the proof may better be provided by finite element numerical analysis.

To interpret the positive geometry condition, we must realize that there is a lower limit on the length, a, of a crack tractable as a crack in a continuum. The crack must be long enough for the continuum description to be valid. Obviously, it cannot be shorter than the fishnet links but, more than that, it cannot be shorter than n-times the size of the RVE of the fishnet underlying the fishnet continuum, with n being about 3 to 6. Thus continuum fishnet cracks make sense only if the rectangular domain of the fishnet is sufficiently large compared to the fishnet RVE, perhaps 20–30 RVE size. This means that a crack in a fishnet continuum makes no sense if it is not longer than about a dozen link lengths.

Instability of fishnet continuum containing a hole

Since the fishnet continuum is governed by the Laplace equation (Eq. (16)), the stress field of the infinite fishnet continuum containing a hole (Fig. 5a) can be obtained by the known solution of an infinite plate containing a hole under antiplane shear loading (Chen et al., 2021). The stress profile along the direction perpendicular to the loading is given by

$$\sigma_y(x) = \sigma[a^2/(a+x)^2 + 1] \tag{38}$$

where σ_0 = far field stress, a = hole diameter, and x = distance measured from the edge of the hole. Due to the formation of the fracture process zone, we may consider that the peak load is attained when the average stress over a fixed distance l_c along this direction reaches a critical value, i.e. $(1/l_c)\int_0^{l_c} \sigma_y(x)\mathrm{d}x = f_t$. It can easily be shown that the peak value of σ would decrease when the hole size a increases. This is an unstable situation and leads to dynamic expansion of the hole (Fig. 5a).

What can we predict for the failure probability of very large fishnets?

Monte Carlo numerical simulations of very large fishnets show that an enclave of several failed links of small length and width forms just before the maximum load. This zone can be treated neither as a crack nor as a circular hole. But both the crack and hole lead to instability and failure once they reach a certain small size. The enclave is an intermediate case between the crack and hole. So it may be inferred that any irregular enclave of failed links of similar size would lead to instability and failure (Fig. 5b)

Now an important point is that in a very large random fishnet the critical irregular enclave of failed links can form at very many different places. That is statistically the same situation as in the weakest link model for a long chain, where the failure of any link leads to the failure of the whole chain. It follows that the distribution of probability P_f of failure of a very large fishnet must be the Weibull distribution, i.e., a straight line in Fig. 7.

Since it appears inconceivable that the slope of the low probability tail in Fig. 7 would decrease compared to smaller fishnets, we must infer that the Weibull modulus of the P_f of a very large fishnet must be $3m$ or larger.

References

Barenblatt, G., 1979. Similarity, Self-Similarity, and Intermediate Asymptotics. Consultants Bureau, New York.

Barenblatt, G., Cherepanov, G., 1961. On brittle cracks under longitudinal shear. J. Appl. Math. Mech. 25 (6), 1654–1666.

Barthelat, F., 2014. Designing nacre-like materials for simultaneous stiffness, strength and toughness: Optimum materials, composition, microstructure and size. J. Mech. Phys. Solids 73, 22–37.

Barthelat, F., Yin, Z., Buehler, M.J., 2016. Structure and mechanics of interfaces in biological materials. Nat. Rev. Mater. 1 (4), 1–16.

Bažant, Z.P., 2002. Scaling of Structural Strength. CRC Press, Boca Raton and New York.

Bažant, Z.P., Le, J.-L., 2009. Nano-mechanics based modeling of lifetime distribution of quasibrittle structures. Eng. Fail. Anal. 16 (8), 2521–2529.

Bažant, Z.P., Le, J.-L., 2017. Probabilistic Mechanics of Quasibrittle Structures: Strength, Lifetime, and Size Effect. Cambridge University Press, Cambridge, U.K..

Bažant, Z.P., Le, J.-L., Salviato, M., 2021. Quasibrittle Fracture Mechanics and Size Effect: A First Course. Oxford University Press.

Bažant, Z.P., Pang, S.-D., 2006. Mechanics-based statistics of failure risk of quasibrittle structures and size effect on safety factors. Proc. Natl. Acad. Sci. 103 (25), 9434–9439.

Bažant, Z.P., Pang, S.-D., 2007. Activation energy based extreme value statistics and size effect in brittle and quasibrittle fracture. J. Mech. Phys. Solids 55 (1), 91–131.
Bažant, Z.P., Planas, J., 1998. Fracture and Size Effect in Concrete and Other Quasibrittle Materials. CRC Press, Boca Raton and New York.
Bouville, F., 2020. Strong and tough nacre-like aluminas: Process–structure–performance relationships and position within the nacre-inspired composite landscape. J. Mater. Res. 35 (8), 1076–1094.
Chen, J.-T., Kao, J.-H., Huang, Y.-L., Kao, S.-K., 2021. On the stress concentration factor of circular/elliptic hole and rigid inclusion under the remote anti-plane shear by using degenerate kernels. Arch. Appl. Mech. 91, 1133–1155.
Daniels, H.E., 1945. The statistical theory of the strength of bundles of threads. I. Proc. R. Soc. Lond. Ser. A Math. Phys. Eng. Sci. 183 (995), 405–435.
Filleter, T., Bernal, R., Li, S., Espinosa, H.D., 2011. Ultrahigh strength and stiffness in cross-linked hierarchical carbon nanotube bundles. Adv. Mater. 23 (25), 2855–2860.
Fisher, R.A., Tippett, L.H.C., 1928. Limiting forms of the frequency distribution of the largest or smallest member of a sample. In: Mathematical Proceedings of the Cambridge Philosophical Society, Vol. 24. Cambridge University Press, Cambridge, U.K., pp. 180–190.
Gao, H., Ji, B., Jäger, I.L., Arzt, E., Fratzl, P., 2003. Materials become insensitive to flaws at nanoscale: lessons from nature. Proc. Natl. Acad. Sci. 100 (10), 5597–5600.
Gumbel, E.J., 1958. Statistics of Extremes. Columbia University Press, New York.
Harlow, D.G., Phoenix, S.L., 1978a. The chain-of-bundles probability model for the strength of fibrous materials I: analysis and conjectures. J. Compos. Mater. 12 (2), 195–214.
Harlow, D.G., Phoenix, S.L., 1978b. The chain-of-bundles probability model for the strength of fibrous materials II: a numerical study of convergence. J. Compos. Mater. 12 (3), 314–334.
Knott, J.F., 1973. Fundamentals of Fracture Mechanics. Butterworth, London, U.K..
Le, J.-L., Bažant, Z.P., 2011. Unified nano-mechanics based probabilistic theory of quasibrittle and brittle structures: II. Fatigue crack growth, lifetime and scaling. J. Mech. Phys. Solids 59 (7), 1322–1337.
Le, J.-L., Bažant, Z.P., Bazant, M.Z., 2009. Subcritical crack growth law and its consequences for lifetime statistics and size effect of quasibrittle structures. J. Phys. D: Appl. Phys. 42 (21), 214008.
Le, J.-L., Bažant, Z.P., Bazant, M.Z., 2011. Unified nano-mechanics based probabilistic theory of quasibrittle and brittle structures: I. Strength, static crack growth, lifetime and scaling. J. Mech. Phys. Solids 59 (7), 1291–1321.
Le, J.-L., Xu, Z., 2019. A simplified probabilistic model for nanocrack propagation and its implications for tail distribution of structural strength. Phys. Mesomech. 22, 85–95.
Luo, W., Bažant, Z.P., 2017a. Fishnet model for failure probability tail of nacre-like imbricated lamellar materials. Proc. Natl. Acad. Sci. 114 (49), 12900–12905.
Luo, W., Bažant, Z.P., 2017b. Fishnet statistics for probabilistic strength and scaling of nacreous imbricated lamellar materials. J. Mech. Phys. Solids 109, 264–287.
Luo, W., Bažant, Z.P., 2018. Fishnet model with order statistics for tail probability of failure of nacreous biomimetic materials with softening interlaminar links. J. Mech. Phys. Solids 121, 281–295.
Luo, W., Bažant, Z.P., 2020. General fishnet statistics of strength: Nacreous, biomimetic, concrete, octet-truss, and other architected or quasibrittle materials. J. Appl. Mech. 87 (3), 031015.
Nguyen, H.T., Pathirage, M., Cusatis, G., Bažant, Z.P., 2020a. Gap test of crack-parallel stress effect on quasibrittle fracture and its consequences. J. Appl. Mech. 87 (7), 071012.
Nguyen, H., Pathirage, M., Rezaei, M., Issa, M., Cusatis, G., Bažant, Z.P., 2020b. New perspective of fracture mechanics inspired by gap test with crack-parallel compression. Proc. Natl. Acad. Sci. 117 (25), 14015–14020.
Tejchman, J., et al., 2013. Modelling the effect of material composition on the tensile properties of concrete. In: Understanding the Tensile Properties of Concrete. Elsevier, pp. 52–97.
Tertuliano, O.A., Greer, J.R., 2016. The nanocomposite nature of bone drives its strength and damage resistance. Nat. Mater. 15 (11), 1195–1202.
Wang, R., Suo, Z., Evans, A., Yao, N., Aksay, I.A., 2001. Deformation mechanisms in nacre. J. Mater. Res. 16 (9), 2485–2493.
Weibull, W., 1939. A statistical theory of the strength of materials. Proc. Royal Swedish Acad. Engrg. Sci. 151, 1–45.
Xu, Z., Le, J.-L., 2018. On power-law tail distribution of strength statistics of brittle and quasibrittle structures. Eng. Fract. Mech. 197, 80–91.
Yin, Z., Hannard, F., Barthelat, F., 2019. Impact-resistant nacre-like transparent materials. Science 364 (6447), 1260–1263.